Simulation of AOT reverse micelles with polyethylenimine in hexane

A. Poghosyan, Stéphane Abel, J. Koetz

Simulation of AOT reverse micelles with polyethylenimine in hexane

A.H. Poghosyan[1], S. Abel[2], J. Koetz[3]

[1]*International Scientific-Educational Center of National Academy of Sciences, M. Baghramyan Ave. 24d, 0019 Yerevan, Armenia*

[2]*Université Paris-Saclay, CEA, CNRS, Institute for Integrative Biology of the Cell, (I2BC), 91198 Gif-sur-Yvette, France*

[3]*Institute for Chemistry, University of Potsdam, 14476 Potsdam, Germany*

Abstract

In this work, we used long (for a total of 2.5 μs) "*all-atom*" molecular dynamics (MD) simulations to investigate the adsorption behaviors of polyethylenimine (PEI) linear chains in Bis(2-ethylhexyl) sulfosuccinate sodium salt (or Aerosol-OT, AOT) reverse micelle (RM) in hexane with a water/AOT molar ratio (W_o) = 30. In absence of PEI chains, the RM is nearly spherical with a micelle radius of ~3.7nm. It takes less than 60 ns for that the PEI starts to unfold and adsorbs in the RM. After 450 ns, the completely unfolded PEI chains are localized at the AOT headgroup region with its nitrogen atoms interacting with the negatively charged headgroup of the AOT. A detailed analysis of the structure of the RM with the PEI reveals that the presence of the polymer chains does not affect significantly the size and shape of this RM with large Wo value which remains close to the results obtained from the MD of the PEI-free RM.

1. Introduction

Colloidal surfactant/polymer mixed systems in both aqueous and non-aqueous solutions have a key potential usage in industry and medicine [1-5] and have been largely studied by means of experimental and computational approaches (see for instance, the reviews [6] and [7] and references cited therein). It is well known that water soluble polyelectrolytes (PEL), which contain anionic or cationic functional groups can interact with oppositely charged individual surfactant molecules below the critical micellization concentration (cmc), and with micelles above the cmc [8,9,10]. Furthermore, PEL can be incorporated into microemulsion droplets and vesicular systems [11-13]. The incorporated polyelectrolytes can tune the interfacial surfactant film [13] and transform vesicles into tube-like structures [14].

In case of water-in-oil microemulsions (reverse micelle, RM) systems with different types of polymers and surfactants have been also reported [15-18]. For instance, the incorporation of the cationic PELs poly(diallyldimethylammonium chloride) PDADMAC and poly(ethyleneimine) (PEI**, Figure 1a**) into sodium dodecyl sulfate (SDS) and sulfobetaine-based (SB) RMs have been studied by Lemke and Koetz [18]. They show that RM can be successfully used for the synthesis of polymer-capped CdS nanoparticles. The effect of

addition of different types of polymers (poly(oxyethyleneglycol - POEG), poly (acrylamide – PAM), poly (vinyl alcohol - PVA), polybutadiene – PBD, poly (propylene glycol - PPG) to water-in-oil (w/o) Bis(2-ethylhexyl) sulfosuccinate sodium salt (AOT, **Figure 1b**) systems has been studied by Suarez and coworkers [15]. They argued that the adding polymer can significantly change the droplet size. The influence of poly (oxyethylene) (POE) on the phase behavior of anionic (AOT) and nonionic ($C_{12}E_5$) surfactant based microemulsions [16]. They report that the large polymers units form droplet clusters.

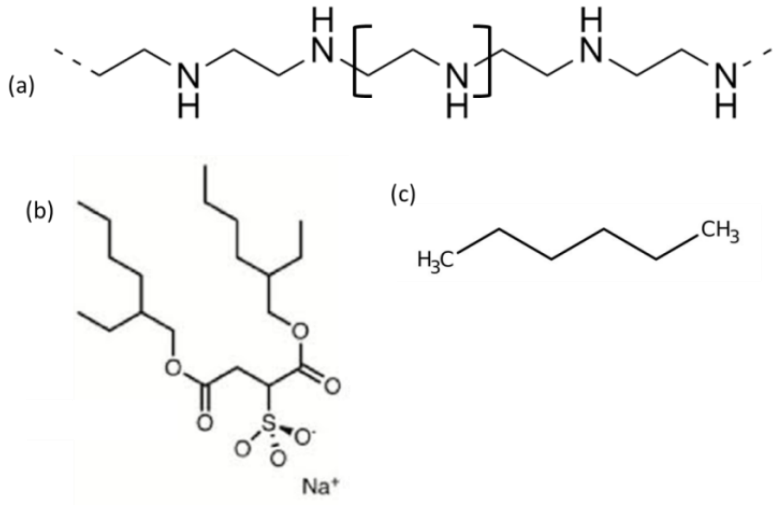

Figure 1: Chemical structures of the molecules simulated in this study. (a) linear polyéthylèneimine (PEI) with its monomer unit (b) Bis(2-ethylhexyl) sulfosuccinate sodium salt (AOT) and (c) hexane.

Among the large variety of polycationic polymers, PEI is a one of most efficient delivery non-viral carriers for gene delivery [19]. The recent developments on design of PEI-stabilized gold clusters in reverse microemulsions [20] and heterocluster-filament formation at the w/o interface of AOT microemulsions demonstrate the importance of PEI-modified soft templates in hierarchical network formation [21,22].

Together with experimental techniques, the computational methods such as molecular dynamics (MD) simulations using a low (e.g., coarse grained, CG) or high resolution (e.g., all-atom/atomistic, AA) molecular models have been shown to be informative and useful tools to investigate such complex systems at the atomic level [23,24] and complement experimental results.Literature of MD studies using CG or AA models of RM is very important and several works, in the following reviews [25,26] have examined the effects of the MD parameters, the size (i.e., Wo (e.g. [27], the force fields [28])and the presence of confined peptides/proteins (e.g. [29,30]) on structure and stability on the overall RM as well as the water pool structure and dynamics (e.g. [26,31]). In case of RM with polymer,there are some MD studies on branched PEI polymer inside of SDS [23] and SB-based [24] reverse micelles. Discussing the conformational features of branched PEI inside of reverse SDS micelles, the authors show that the size and shape of sphere-like inverse micelles depends

on incorporated branched PEI [23]. The localization of branched PEI inside of droplet depends on type of surfactant, that is to say in case of anionic surfactant, PEI is localized at the headgroup region, where the polymer nitrogen atoms are close to SDS sulfur atoms [23], while in zwitterionic SB-based micelles, the branched PEI undergoes a conformational change and finally is located in the center of water droplet [24].

As mentioned earlier, the anionic AOT surfactant is known to form RM assemblies in various alkanes [32], ionic liquids (see for instance [33] and references cited therein) solvents and even in absence of water [34]. The RM and confined water structural properties depend on various experimental parameters and among them the water content inside the RM interior as a function of the AOT concentration (i.e., the water-to-surfactant ratio, W_o) [35-37]. The aim of this present work is to provide additional insights into the interactions of the PEI chains with a model of large AOT RM (W_0=30) in hexane and in addition to our previous MD done with SDS/SB RMs [23,24], Detailed information about localization and orientation of PEI and its influence on the RM structure. This MD data will be important for understanding of the character of electrostatic interactions, as such kind of polymer-reverse micelle complexes use as a template for nanocrystals formation [23,24].

2. Construction and simulation details

For this work, we used *all-atom* MD simulations to have detailed information about the structure and interactions of the PEI chain with the AOT RM. The building of final atomistic quaternary system containing the AOT/PEI/H_2O/hexane was done after the construction and the equilibration of each component separately (i.e., AOT RM (step 1) and the PEI chains (step 2) in hexane solvent separately). This is detailed in the next paragraphs.

2.1 Step 1 – Construction of the pre-assembled model of Reverse AOT RM. A pre-assembled atomistic model of the AOT RM with W_o=30 was built with a PDB structure of the AOT taken from our previous work [38,39] using the Packmol package [40] with 150 AOT, Na^+ ions and 4500 water molecules. Briefly, a water sphere consisting of 4500 water molecules and 150 sodium ions was created. The radius water core was set to 32 Å, with an effective volume of water of ~30$Å^3$. 150 AOT molecules, where then around water core with AOT tails pointed outward. The resulting micelle was minimized via steepest descent algorithm (5000 steps) and equilibrated at constant temperature (NVT ensemble). The RM was then placed into the center of a cubic box of 10x10x10nm^3 filled with 2859 hexane taken from a pre-equilibrated small box of 128 hexane molecules equilibrated at ambient temperature and pressure conditions. The resulting ternary RM system was then subjected to energy minimization followed by short simulation under NVT and NPT ensembles at 298K and 1atmto reach to desired temperature and density. We applied position restraining (1000kj/mol) to AOT/water/Na^+ during the equilibration stages to well equilibrated the hexane around the RM.

2.2 Step 2 Construction of the Polyethylenimine in hexane. For this work, we simulated 3 linear PEI chains with 100 monomer units each for an overall molecular weight of ~12KDa. The molecular model of the PEI was built with the *Polymer Builder* module of CHARMM-GUI (https://charmm-gui.org/?doc=input/polymer) [41,42]. The chains were then the inserted in a hexane box of 7.7x7.7x7.7nm^3 filled with 1700 hexane molecules. The system was also subjected to energy minimization by steepest descent method and a short NVT simulation was done after production run of 500ns. As with the RM system, we applied position restraining (1000kj/mol) to polymer chains during the equilibration stages to well equilibrate the hexane around the polymer.

2.3 Step 3- Construction of the reverse AOT RM with PEI in hexane. Finally, we put the last configurations of RM and the PEI chains from the above systems into a box of 12.5x12.5x12.5nm^3 filled with 7210 hexane molecules. The PEI polymer chains were placed manually at 3 nm of the RM surface (i.e., with a center of mass distance between the RM and PEI of ~6.0 nm). The resulting systems was then subjected to geometric optimization and small NVT and NPT runs at room temperature with the AOT RM and PEI chains kept fixed with position restrains (1000kj/mol). This final system was then simulated twice (called hereafter "Replica") in the NPT ensemble to be well in the lab conditions during 1000ns each with different starting conditions to have enough statistics.

2.4 Simulation details. To model the AOT and Na^+, we used the "*all-atom*" CHARMM27 force field [43] with the simple point of charge (SPC) [44] water model. The PEI chain was modeled using the CGenFF parameters taken from CHARMM-GUI [41,42]. The Nose-Hoover [45] and Parrinello-Rahman [46] thermostat and barostat (with t_T and t_P values of 1.0 and 5.0 ps, respectively) were used to regulate the temperature and pressure, respectively, and set to 298K and 1 atm. The electrostatic interactions were computed with the particle mesh Ewald (PME) method [47] with a cutoff of 1.2nm, and the van-der-Waals interactions were smoothly switched off at 1.0-1.2nm by a force-switching function [48]. The LINCS [49] algorithm was used to constrain the bonds to their equilibration values. The periodic boundary conditions were applied in all directions. The timestep was set to 2fs throughout the production run and the atomic coordinates of the systems saved every 10000 steps (20ps) for subsequent analysis of the RM and PEI properties. All the simulations and analysis were carried out using the latest version of GROMACS package with GPU support [50,51] on our workstations [52] and snapshots prepared with the PyMOL [53] and VMD [54] programs.

3. Results and discussions

3.1 Pre-assembled AOT RM in hexane. We start our analysis by examining the structural changes of the RM size and shape without the PEI along the 1000 ns of simulation time. As

previously (for instance in refs. [43] or in [55]) to describe, the overall RM and water core sizes, we computed their radius of gyration, R_g with the following equation [55].

$$R_g^2 = \frac{1}{2n^2}\sum_{i=1}^{n}\sum_{j=1}^{n}\left\langle (r_{ij})^2 \right\rangle = \frac{1}{n}\sum_{i=1}^{n}\langle (r_{ic})^2 \rangle \quad (1)$$

where n is the number of atoms, n_{ij} is the distance between atom i and j, and r_{ic} is the distance between atom i and the center of mass (C.O.M) of the RM. $\langle \ldots \rangle$ is the ensemble average.

In **Figure 2**, we plotted the time evolution of the $R_g$for different regions which characterize the RM [43], i.e., the water R_g^w, $R_g^{AOT-w}$and R_g^{AOT}, by including in the equation 1, only the water, AOT-water, and only AOT atoms, respectively.

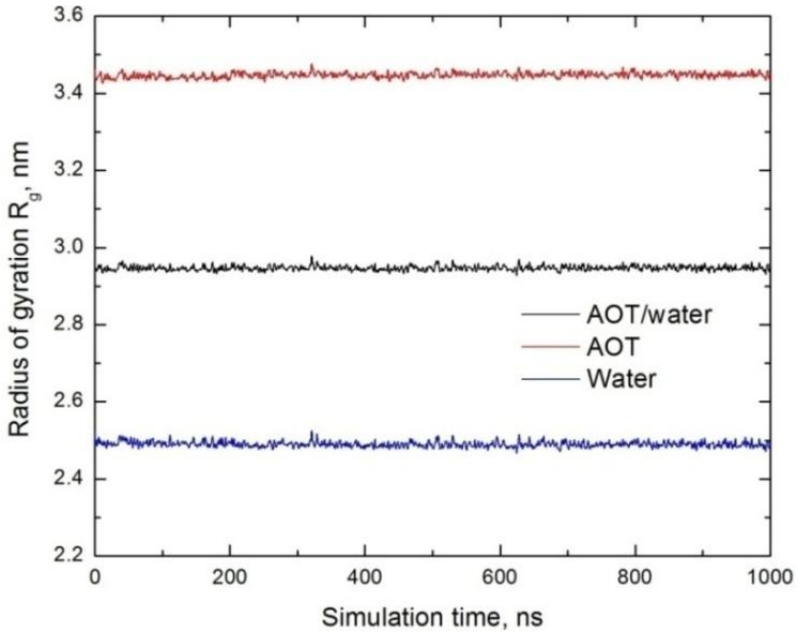

Figure 2: The time evolution of the radius of gyration including the overall RM, AOT and water

As we can see with this Figure, these three quantities do not show any drifts and are stable during the simulation time period, indicating that the RM and water core sizes do not vary during the course of the run and are, on average, equal to 2.49 ± 0.01, 2.94 ± 0.01 and 3.44 ± 0.01nm and respectively. Comparison of the MD results with experiments is often difficult for RM, since the surfactant concentration in MD is significantly larger (here, 250 mM) than in experiments (for instance, 0.1 M in ref. [56]) and that we simulated only one aggregate (and therefore not interactions between aggregates are taken into account). For instance, the experimental value of radius of gyration obtained from by neutron spin echo and SR-SAXS [56,57] of AOT RM with W_0=30 in similar solvent (heptane) is found to be ~4.2nm [56].

The time evolution of the mean distances between RM COM-sulfur and COM-AOT's terminal carbon atoms averaged over all AOT molecules were also computed and plotted in **Figure S1**. These two distances are also found stable during the courses of the simulations and are equal to ~3.1 and 3.7nm, respectively. Note that the distances between the C.O.M and sulfurs AOT-terminals carbons can be considered as similar to as average distance from the RM outermost waters, i.e.; R_W and the radius of whole micelle $R_M$and not far to the experimental RM hydrodynamic radius R_H obtained with, for instance, dynamical light scattering (DLS) for a spherical aggregate as found for our models [58]. From theR_M and $R_W$difference, it is also possible to have a (rough) estimation of the thickness of the AOT hydrophobic ethylexyl chains (0.6 nm), This is 2 times lower than the value of the chains in its extended conformation [43], indicating that they are folded.

The next step of the analysis of the RM structural properties is to examine the overall shape of the RM using the computation of the three principal moments of inertia, I_1, I_2 and I_3 and the eccentricity (*ecc*) (also called «sphericity») using the equations 2 and 3, respectively [43]. We approximate the RM as an ellipsoid of uniform density and the moments of inertia, can obtain three semi-axes lengths, *a*, *b*and *c* of the RM with the equation 3[43]:

$$I_1 = \frac{1}{5} M_T (a^2 + b^2)$$
$$I_2 = \frac{1}{5} M_T (a^2 + c^2) \quad (2)$$
$$I_3 = \frac{1}{5} M_T (b^2 + c^2)$$

$$ecc = 1 - \frac{I_{min}}{I_{avg}} \quad (3)$$

Where$M_T$is the total mass of the RM (including the AOT molecules, water and Na^+ ions),I_{min} is the smallest value of the moment of inertia (with $I_1 > I_2 > I_3$)along all axis and I_{avg} is the average of all three moments of inertia. Note that the eccentricity is zero for a perfect spherical case. The time variation of the eccentricity is shown in **Figure 3** with two snapshots of the RM at the minimum and maximum values of *ecc*. The micelle shape is found very stable with *ecc* value around 0.06 indicating that the RM can be considered, on average, during the run as a quasi-spherical aggregate. This is confirmed by the close average values of three semi-axe lengths *a*, *b* and *c* which are equal to 3.53 ± 0.01, 3.76 ± 0.01 and 4.01 ± 0.01 nm, respectively. Note that AOT reverse micelles found to be spherical by covering a wide range of W_0 [59,60].

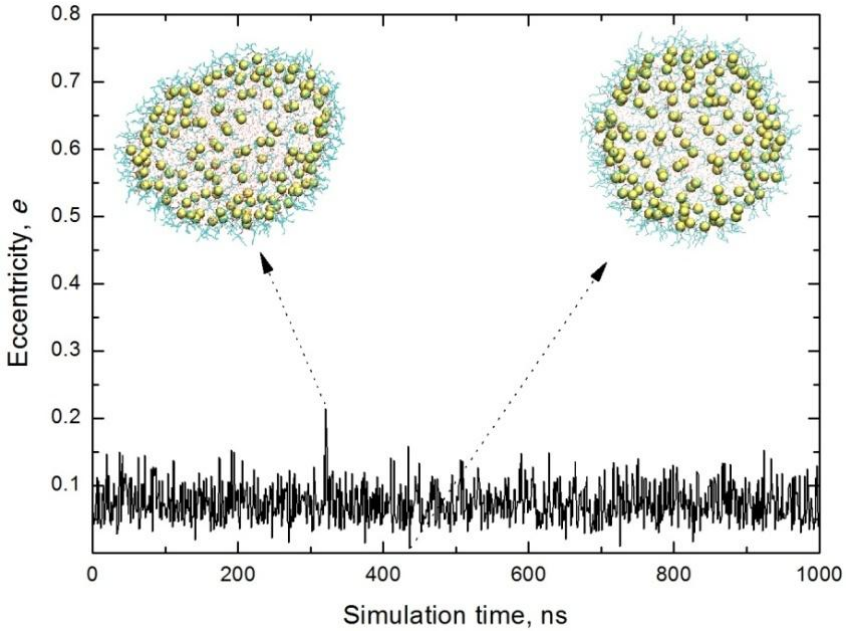

Figure 3: Time evolution of the eccentricity of the overall RM. The water and sulfur atoms of the AOT are shown in red points and yellow CPK spheres. The blue lines at the micelle surface delimit the alkyl chain of the AOT.RM rendered with the VMD program [54].

Finally, we computed, the translational diffusion D_{RM} of the RM from the linear fitting of mean square displacement (MSD) versus time starting from different time points. We obtained a mean value D_{RM} around ~0.95 ± 0.01x10^{-7} cm/s, which is close to the experimental value of ~10^{-7}cm/s [61] for a RM with the same size and in the same solvent.

3.2 Polyethylenimine in hexane. The simulations in this work also provided some insights into the structure of the PEI chains in hexane. The computed radii of gyration of three chains and the overall chains of the PEI as a function of the 500 ns simulation time (**Figure 4**). Despite large fluctuations in the middle of simulation of the PEI R_g, no significant structural changes of the PEI chains are observed during the course of the 500 ns of the MD run. The R_g, computed from the last 100 ns where the R_g fluctuations are reduced is equal to 1.3 ± 0.2nm. Simultaneously, the end-to-end distance (d_{ee}) was also calculated (data not shown) to monitor the d_{ee}/R_g ratio for freely-joint model, introduced by Flory [62]. The analysis of data shown that the mean d_{ee}/R_g ratios for the three chains (obtained by averaging all the chains from last 100ns of production run) are: 2.27 ± 0.18; 2.03 ± 0.21 and 1.91 ± 0.17 and deviate from ideal chain which should be ~2.45.

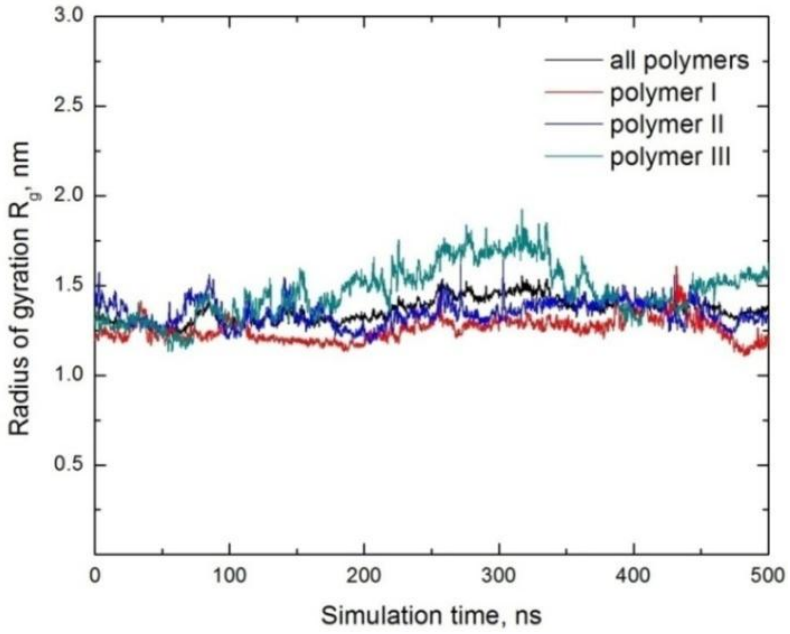

Figure 4. The radii of gyration of PEI depending on simulation time.

Another approach to demonstrate an effective size of polymer is the mean distance from center of mass of PEI and the nitrogen atoms of the polymer. The corresponding plot is shown in **Figure S2 in SI,** with an average value of ~1.95 ± 0.02nm. To obtain information of the shape of polymer, we have also calculated the sizes of folded polymer by determining the minimum and maximum distances between PEI nitrogen atoms. A visual inspection of trajectories shows that the folded polymer has nearly ellipsoidal shape with mean values for the x and y axis of ~4.4 ± 0.1nm and 1.2 ± 0.1nm. The corresponding snapshot extracted from last frame of trajectory was shown in **Figure S3 in SI**.

3.3 Reverse AOT micelle and PEI in hexane. Before to discuss the results, we provide in **Figure 5,** two illustrative snapshots extracted at t=0 and 1000 ns of the trajectory for the first replica (see also **Figure S4 in SI** for last snapshot of the second replica). Other snapshots (**Figure 6**) from the first Replica_1 simulation also provides an illustration of the time evolution of the absorption of the PEI into the RM. From these figures, one can see that the two replicas give similar results and at first 45 ns of the two runs, the polymer C.O.M remains far (~6-8nm) from the RM (close to its initial position) and after that time point, the polymer aggregate starts to come closer to AOT RM. It took approximatively 60 ns for that polymer starts to unfold and absorbs to RM surface forming a pore inside the AOT. The polymer chains are completely unfolded a t=100 ns with a large part of the chain residing in the water core but it needs few hundreds of ns of MD for that the polymer chains migrate to the RM interfacial region delimited by the AOT headgroup (see **Figures 5 and 6**). We note that during the PEI adsorption process, large deformation of the RM occurs (see for instance snapshot at t=66 ns **in Figure 6**) but the RM becomes quasi-spherical again after the chain is

permanently located and stabilized in the interfacial region. Similar behavior is observed for the second replica (not shown).

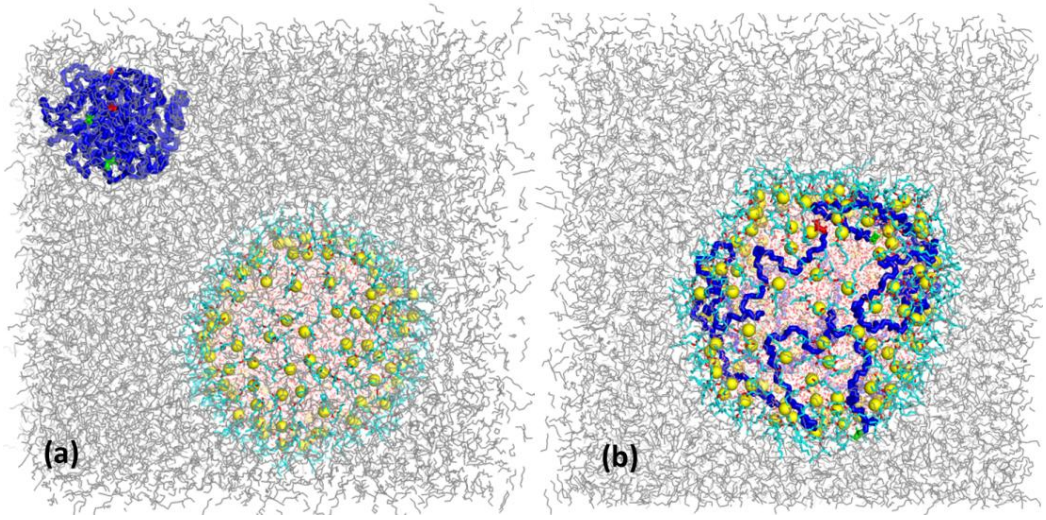

Figure 5: The snapshots from starting (a) and ending (1000ns) (b) configurations of reverse AOT micelle/PEI in hexane for the first replica (see also **Figure S4** in the SI for the second replica). The atoms are represented as follows: AOT sulfur – yellow (vdW), carbon –cyan, polymer – blue - (tube). The hexane molecules are colored in gray (points). The beginning and ending monomers of they are colored in red and greens colors respectively using PyMol [53].

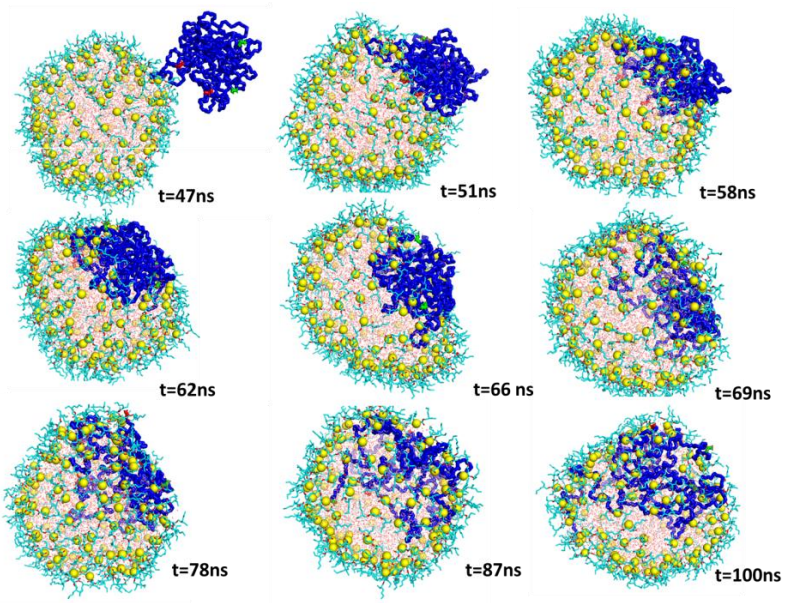

Figure 6: The snapshots from simulation at different time point indicating the polymer entering procedure for the first replica. PEI chains are colored in red and greens colors respectively using PyMOL [53].

To examine the adsorption dynamics of the PEI in the RM, we have firstly calculated the time evolution of the distance between the RM and polymer C.O.M.s(all atoms of polymer were included to calculate C.O.M.) for the two runs (**Figure S5 in the SI**)and the shape parameters as for the PEI free micelle by *not* taking into account the polymer chain in the calculation for the two replicas (**Table S1 in the SI)**.Consistent with **Figure S5**, we show that PEI adsorption into RM are similar in the two replicas: at around 50 ns and leads to negligible increase (around 0.1 nm) of the RM three R_g values (**Figure 7**) with average values for theR_g^w, R_g^{AOT-w} andR_g^{AOT}(computed from the last 100 ns using the same approach as above) of ~2.53 ± 0.01, 3.20 ± 0.01 and ~3.58 ± 0.01nm, respectively.

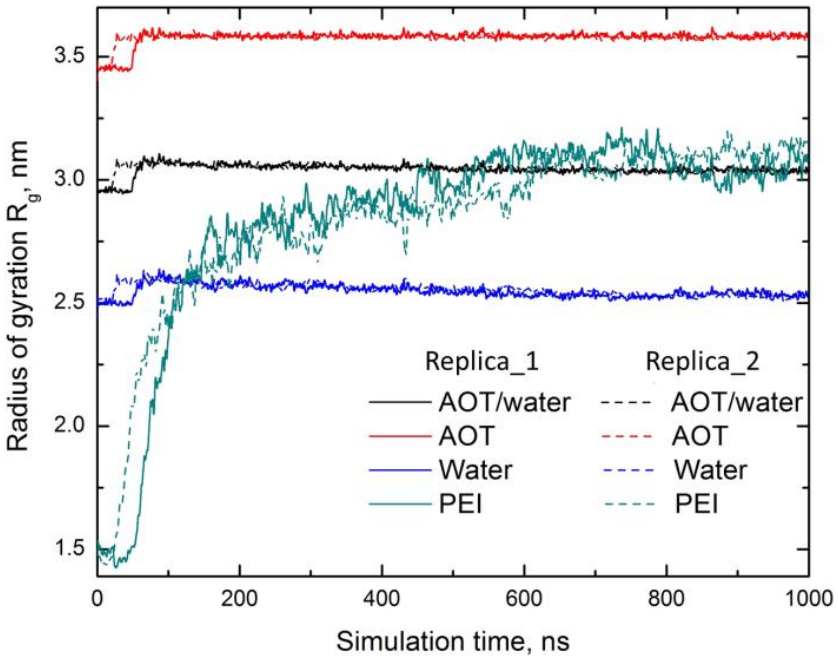

Figure 7: The radius of gyration depending on simulation time obtained for the two replicas.

In addition, we found for the two replicas that the AOT hydrophobic thickness is closely to the value found in the polymer-free RM (~0.65nm) indicating that the PEI localization does not affect the folding of the AOT alkyl chain.

In case of the micelle shape parameters, the average three semi-axes lengths and *ecc* obtained for the two replicas show a small increase and are equal to 3.60, 3.87 and 4.16 nm and 0.07, respectively. These values are 2.0 %, 3.0 %, 3.6 % and 10.0 % higher than the respective values found for the overall PEI free RM indicating a negligible deformation the RM with the presence of the polymer.

To better visualize of the localization of encapsulated PEI into the RM, we computed mean radial density profiles along the distance to the RM center-of-mass for the AOT sulfur and

the nitrogen atoms of PEI after the 600 ns of the run of the two replicas (**Figures 8** and **S6**) using the equation 4 [43].

$$N_a(r)dr = \left\langle \sum_i \partial(r_{com} - r_i) \frac{1}{4\pi r^3} \right\rangle \qquad (4)$$

where the sum extends to all the atoms of the component a and ⟨...⟩ is the ensemble average. The density profiles were computed with respect to the RM center of mass ($r_{com} = 0nm$).

For AOT sulfurs, we found a peak at about ~3.2nm from micelle center, close to the RM radius computed above. The RDF curve of PEI nitrogen atoms also exhibits a peak at ~3.0nm of the RM COM, which is almost the same as the position of the AOT sulfurs indicating that the PEI monomers reside at the headgroup-water interface at a close distance close contact to the ATOM sulfur atom. This is also confirmed with the visual inspection of trajectory or the computed percentage (95%) of PEI monomers that reside at 0.2 nm of the AOT headgroup. Similar result was reported by us for SDS RM that has a similar headgroup [23] and contrast with PEI in RM with zwitterionic surfactant [24].

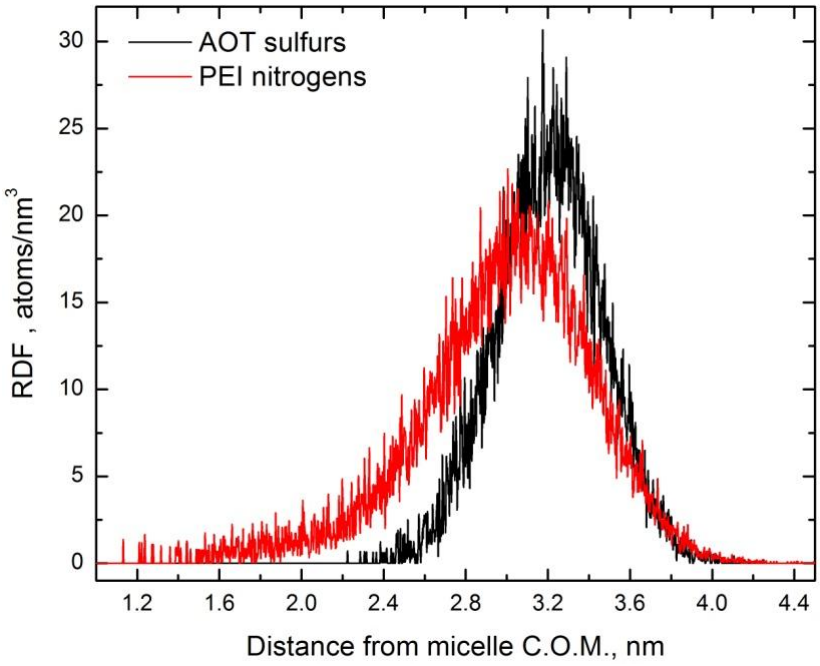

Figure 8: The RDF of sulfurs and nitrogen atoms from center of mass of micelle. See **Figure S6** in SI

Finally, by tracking the behavior of water molecules, we conclude that almost no water molecules are flowing to the hexane media during whole simulation run (data not shown), however, in case of SDS and SB-based micelles a small amount of water molecules are migrates from interior to oil media [23,24].

4. Conclusion

In this paper, we carried out microseconds atomistic MD simulations to investigate the influence of the adsorption of PEI chains in a large model of AOT RM in hexane with W_0 of 30. The MD results performed with two replicas obtained from different starting conditions show that it took approximately 60 ns for that the PEI chains absorb into the RM by forming a pore in the RM surface. During the adsorption process, the PEI chains unfold and deform significantly the RM at the beginning of adsorption process. With the encapsulated PEI chains, the AOT RM size and shape properties are not significantly affected since we observed a non-significative increase of the micelle size (0.15 nm) and (eccentricity around 0.07). Inside the RM, the PEI chains are unfolded in contrast to in bulk hexane when the chains form a stable and compact aggregate. Similarly, to other anionic RM system (such as SDS), the PEI chains reside at the AOT-water interface close to the AOT sulfur atoms.

Acknowledgements

The research has been partly funded by the Science Committee project (SCSMESCS RA - 21T-1B110) (A.H.P). We also acknowledge computational resources provided at the Institute for Informatics and Automation Problems of NAS RA, Armenia.

Compliance with ethical standards

Conflict of interest: The authors declares that they have no conflict of interest.

5. References

[1] C.T. Kwak (Ed.), Polymer-surfactant systems (Surfactant Science series; v. 77), Marcel Dekker Inc., New York Basel· Hong Kong, 1998.

[2] D. Myers (Ed.), Surfactant science and technology, VCH Publishers, Weinheim, 1992.

[3] J. Kreuter (Ed.) Colloidal drug delivery systems, Marcel Dekker Inc., New York Basel · Hong Kong, 1994.

[4] Kalal J, Drobnik J, Kopecek J, Exner J. Water soluble polymers for medicine. *British Polymer Journal*. 1978;10(2):111–114

[5] Farokhzad OC, Langer R. Impact of nanotechnology on drug delivery. *ACS Nano*. 2009;3(1):16–20.

[6] B. Lingman , F. Antunes, S. Aidarova, M. Miguel, T.Nylanger. Polyelectrolyte-surfactant association-from fundamentals to applications. Colloid Journal, 2014, 76(6):585-594

[7] J.J.Madinya, C.E.Sing. Hybrid field theory and particle simulation model of polyelectrolyte-surfactant coacervation. Macromolecules. 2022, 55(6):2358-2373

[8] H. Dautzenberg, W. Jaeger, J. Kötz, B. Philipp, Ch. Seidel, D. Stscherbina, Polyelectrolytes – Formation, characterization and application, Hanser Publishers, Munich ·Vienna·New York, 1994.

[9] B. Philipp,H.Dautzenberg, K.-J. Linow, J. Kötz, W. Dawydoff, Polyelectrolyte complexes – Recent developments and open problems, Prog. Polym. Sci. 1989, 14, 91-172.

[10] A.E. Aferni, M.Guettari, M. Kamli, T.Tajouri, A.Ponton . A structural study of polymer-surfactant system in dilute and entangled regime: Effect of high concentrations of surfactant and polymer molecular weight. J. Mol. Str., 2020, 1199, 127052

[11] T. Beitz, J. Kötz, S. Friberg, Polymer-modified ionic microemulsions formed in the system SDS/water/xylene/pentanol, Prog. Colloid Polym. Sci. 111 (1998) 100–106.

[12] C. Note, S. Kosmella, J. Koetz, Structural changes in poly(ethyleneimine) modified microemulsion, J. Colloid Interface Sci. 302 (2006) 662–668.

[13] M. Fechner, J. Koetz, Polyampholyte-surfactant film tuning in reverse microemulsions, Langmuir 2011, 27, 5316-5323.

[14] A. Köth, D. Appelhans, D. Robertson, B. Tiersch, J. Koetz, Use of weakly cationic dendritic glycopolymer for morphological transformation of phospholipid vesicles into tube-like network, Soft Matter 2011, 7, 10581-10584.

[15] M.-J. Suarez, H. Levy, J. Lang. Effect of addition of polymer to water-in-oil microemulsions on droplet size and exchange of material between droplets. J. Phys. Chem. 1993, 97, 9808-9816

[16] W. Meier, Poly(oxyethylene) adsorption in water/oil microemulsions: a conductive study, Langmuir 12 (1996) 1188–1192

[17] A.H. Poghosyan, L.H. Arsenyan, H.H. Gharabekyan, S. Falkenhagen, J. Koetz, A.Shahinyan, The molecular dynamics simulation of inverse sodiumdodecylsulfate (SDS) micelles in toluene/pentanol solute in absence and presence of poly(diallyldimethyl ammonium chloride), J. Colloid Interface Sci.358 (2011) 175–181.

[18] K. Lemke, J. Koetz, Polycation capped CdS quantum dots synthesized in reverse microemulsions, J. Nanomater. (2012) (ID 478153). DOI:10.1155/2012/478153

[19] M.A. Mintzer, E.E.Simanek. Nonviral vectors for gene delivery, Chem. Rev. 2009, 109(2), 259-302

[20] K. Lemke, C. Prietzel, J. Koetz, Fluorescent gold clusters synthesized in a poly(ethyleneimine) modified microemulsion, J. Colloid Interface Sci. 394 (2013) 141–146.

[21] R.F. Martin, C. Prietzel, J. Koetz, Template-mediated self-assembly of magnetite -gold nanoparticle superstructures at the water-in-oil interface of AOT reverse microemulsions. J. Coll. and Int. Sci, 2021, 581, 44-55.

[22] R.F. Martin, A. Thünemann, J.M. Stockmann, J. Radnik, J. Koetz, From nanoparticle heteroclusters to filament networks by self-assembly at the water-oil interface of reverse microemulsions, Langmuir, 2021, 37, 8876-8885.

[23] Poghosyan A.H., Arsenyan L.H., Shahinyan A.A., Koetz J. "Polyethyleneimine Loaded Inverse SDS Micelle in Pentanol/Toluene Media", *Colloids and Surfaces A: Physicochemical and Engineering Aspects.* **2016,** 506(2):402-408

[24] Poghosyan A.H.,Arsenyan L.H., Antonyan L.A., Shahinyan A.A., Koetz J. "Molecular dynamics simulations of branched polyethyleneimine in water-in-heptanol micelles stabilized by zwitterionic surfactants", *Colloids and Surfaces A: Physicochemical and Engineering Aspects.* **2015.** 479:18-24.

[25] Arsene, M.-L.; R˘aut, I.;C˘alin, M.; Jecu, M.-L.; Doni, M.;Gurban, A.-M. "Versatility of Reverse Micelles: From Biomimetic Models to Nano (Bio)Sensor Design". *Processes***2021**, 9, 345.

[26] Eskici G., Axelsen P.H. "The Size of AOT Reverse Micelles" *J. Phys. Chem. B* **2016**, 120, 44, 11337–11347

[27] A. Siddiqim, C. Herdes, "Water effect in the reverse micellar formation of docusate sodium. A coarse-grained molecular dynamics approach", *Fluid Phase Equilibria*, Volume 559, August **2022**, 113469

[28] A. V. Martinez, L. Dominguez, E. Małolepsza, A.Moser, Z. Ziegler, and J.E. Straub, "Probing the Structure and Dynamics of Confined Water in AOT Reverse Micelles", *J. Phys. Chem. B* **2013**, 117, 24, 7345–7351

[29]M. Senske, Y. Xua, A. Bäumer, S. Schäfer., H. Wirtz, J. Savolainen, H. Weingärtner, M. Havenith,"Local Chemistry of the Surfactant's Head Groups Determines Protein Stability in Reverse Micelles", *Phys. Chem. Chem. Phys.*, **2018**,20, 8515-8522

[30] A. V.Martinez, S. C. DeSensi, L. Dominguez, E. Rivera, and J. E. Straub, “Protein folding in a reverse micelle environment: The role of confinement and dehydration”, *J. Chem. Phys.* 134, 055107 (**2011**)

[31]A. Baksi, P. Kr. Ghorai, and R. Biswas, “Dynamic Susceptibility and Structural Heterogeneity of Large Reverse Micellar Water: An Examination of the Core−Shell Model via Probing the Layer-wise Features”, *J Phys Chem B*. **2020** Apr 9;124(14):2848-2863.

[32] Abluin E., Lissi E., Duarte R., Silber J.J., Biasutti M.A., Solubilization in AOT-water reverse micelles. Effect of external solvent. Langmuir, 2002, 18, 8340-8344

[33] N.M. Correa, Silber J.J., Riter R.E., Levinger N.E. Nonaqueous polar solvents in reverse micelle systems. Chemical Reviews, 2012, 112(8), 4569-4602

[34] R. Urano, G.A. Pantelopulos, J.E. Straub. Aerosol-OT surfactant forms stable reverse micelles in apolar solvents in the absence of water. J. Phys. Chem. B., 2019, 123, 2546-2557

[35] N.E. Levinger, L.A. Swafford, Ultrafast dynamics in reverse micelles. Annu. Rev.Phys. Chem., 2009, 60, 385-406

[36] M.D. Fayer, N.E. Levinger, Analysis of water in confined geometries and at interfaces, Annu. Rev. Anal. Chem. 2010, 3:89-107

[37] D.E. Moilanen, E.E. Fenn, D. Wong, M. Fayer, Water dynamics in large and small reverse micelles: From two ensembles to collective behavior. J. Chem. Phys., 131, 2009, 014704

[38] Poghosyan A.H., Shahinyan A.A., Koetz J. “Self-assembled monolayer formation of distorted cylindrical AOT micelles on gold surfaces”, Colloids and Surfaces A: Physicochemical and Engineering Aspects. 2018, 546(5):20-27;

[39] Poghosyan A.H., Adamyan M. P., Shahinyan A.A., Koetz J. “AOT Bilayer Adsorption on Gold Surfaces: A Molecular Dynamics Study”, The Journal of Physical Chemistry B. 2019, 123(4):948-953.

[40] Martinez, L.; Andrade, R.; Birgin, E.G.; Martínez, J.M. PACKMOL: A package for building initial configurations for molecular dynamics simulations. J. Comput. Chem. 2009, 30, 2157–2164.

[41] S. Jo, T. Kim, V.G. Iyer, and W. Im “CHARMM-GUI: A Web-based Graphical User Interface for CHARMM”. J. Comput. Chem. 2008, 29:1859-1865

[42] Y.K. Choi, S-J. Park, S. Park, S. Kim, N.R. Kern, J. Lee, and W. Im ”CHARMM-GUI Polymer Builder for Modeling and Simulation of Synthetic Polymers”. J. Chem. Theory Comput. 2021, 17:2431–2443

[43] Abel S, Sterpone F, Bandyopadhyay S, Marchi M. Molecular Modeling and Simulations of AOT-Water Reverse Micelles in Isooctane: Structural and Dynamic Properties. *J Phys Chem B*. **2004**;108, 19458–19466.

[44] H.J.C. Berendsen, J.P.M. Postma, W.F. van Gunsteren, J. Hermans, Interaction models of water in relation to protein hydration, Intermolecular forces (1981) 331-342

[45] S.Nosé, A unified formulation of the constant temperature molecular-dynamics methods, J. Chem. Phys. 81 (1) (1984) 511–519.

[46] A. Rahman, N. Parrinello, Polymorphic transitions in single crystals: a new molecular dynamics method, J. Appl. Phys. 52 (1981) 7182–7189.

[47] T. Darden, D. York, L. Pedersen, 1993. Particle mesh Ewald: anN·log(N) method for Ewald sums in large systems, J. Chem. Phys. 98, 10089.

[48] P.J. Steinbach, B.R. Brooks, New spherical –cutoff methods for long-range forces in macromolecular solution. J. Comp.Chem., 1994, 15(7):667-683

[49] B. Hess, H. Bekker, H.J.C. Berendsen, J. Fraaije, LINCS: a linear constraint solver for molecular simulations, J. Comput. Chem. 18 (1987) 1463–1472.

[50] H.J.C.Berendsen, D. van der Spoel, R. van Drunen, GROMACS: a message-passing parallel molecular dynamics implementation, Comput. Phys. Commun. 91 (1995) 43–56;

[51] Abraham, M.J.; Murtola, T.; Schulz, R.; Páll, S.; Smith, J.C., Hess, B., Lindahl, E. GROMACS: High performance molecular simulations through multi-level parallelism from laptops to supercomputers. SoftwareX 2015, 1, 19-25.

[52] Poghosyan A.H., Astsatryan H.V., Shahinyan A.A. “Parallel Peculiarities and Performance of GROMACS Package on HPC Platforms”, *International Journal of Scientific and Engineering Research.* **2013**, 4(12):1755-1761.

[53] DeLano, W. L. The PyMOL Molecular Graphics System 2.4; Schrödinger, LLC, April 2020

[54] W. Humphrey, A. Dalke, K. Schulten, VMD: visual molecular dynamics, J. Mol. Graph. 14 (1996) 33–38.

[55] G. Eskici, P.H. Axelsen. The size of AOT reverse micelle. J.Phys. Chem. B., 2016, 120, 11337-11347

[56] M. Hirai, R.K.Hirai, H.Iwase, S.Arai, S.Mitsuya, T.Takeda, H.Seto, M.Nagao, “Dynamics of w/o AOT microemulsions studied by neutron spin echo”. J. Phys. Chem. Solids, 66 (1999), 1359-1361;

[57] M. Hirai, R.Kawai-Hirai, M. Sanada, H. Iwase, S.Mitsuya, “Characterics of AOT microemusion structure dynamics depending on apolar solvents”, J. Phys. Chem. B., 103 (1999), 9658-9662

[58] P.A. Hassan, S.Rana, G. Verma, Making sense of Brownian motion: Colloid characterization by dynamic light scattering. Langmuir, 2015, 31(1), 3-12

[59] S. Tovstun, V.F. Razumov, What makes AOT reverse micelles spherical?. Coll. and Pol. Sci., 2014, 293(1):165-176.

[60] S.A. Kislenko, V.F. Razumov. Molecular dynamics study of micellization thermodynamics in AOT/hexane system. Colloid Journal, 2017, 79(1):76-80

[61] C.L. Mesa, L. Coppola, G.A. Ranieri, M. Terenzi, Chidichimo G. Phase diagram and phase properties of the system water-hexane-Aerosol OT, Langmuir, 1992, 8, 2616-2622

[62] P.J. Flory, Statistical Mechanics of Chain Molecules, Wiley, New York, 1969